



pH 敏感铱、钌和铂配合物在肿瘤靶向荧光成像和治疗中的应用

张思琪¹ 高丽华² 赵 华² 王克志^{*1}

(¹ 北京师范大学化学学院, 放射性药物教育部重点实验室, 北京 100875)

(² 北京工商大学理学院, 北京 100048)

摘要: 肿瘤组织的微酸性环境为肿瘤准确诊断和有效治疗提供了新思路。pH 敏感性金属配合物因具有较高的物理化学稳定性, 突出的光谱特性和肿瘤靶向性等性质, 引起高度关注。本文综述了这种肿瘤酸性微环境的产生机制以及近年来对这种酸性微环境敏感的铱、钌、铂配合物作为肿瘤成像和治疗试剂的研究进展。

关键词: 金属配合物; pH 敏感性; 肿瘤成像; 肿瘤治疗

中图分类号: O614.82⁵; O614.82¹; O614.82⁶ 文献标识码: A 文章编号: 1001-4861(2019)11-1974-13

DOI: 10.11862/CJIC.2019.231

pH-Sensitive Iridium, Ruthenium and Platinum Complexes for Tumor-Specific Fluorescence Imaging and Cancer Therapy

ZHANG Si-Qi¹ GAO Li-Hua² ZHAO Hua² WANG Ke-Zhi^{*1}

(¹Key Laboratory of Radiopharmaceuticals, Ministry of Education,

College of Chemistry, Beijing Normal University, Beijing 100875, China)

(²School of Science, Beijing Technology and Business University, Beijing 100048, China)

Abstract: Acidic pH in tumor tissues provides a powerful platform for accurate tumor diagnosis and efficient therapy. The pH-sensitive iridium, ruthenium and platinum metal complexes have attracted increasing attention due to their high physicochemical stability, favorable spectral properties and tumor targetability. In this review, we summarize formation mechanisms of the acidic tumor microenvironment and recent advances on the acidic microenvironment-sensitive metal complexes of iridium, ruthenium and platinum for tumor imaging chemotherapy agents.

Keywords: metal complex; pH sensitive; tumor imaging; tumor therapy

0 Introduction

Cancer has become the second leading cause of death followed by ischemic heart disease and it is predicted that new cancer cases will increase more than 27 millions by 2030^[1]. Chemotherapy and image-

guided surgery are still the most commonly used methods for cancer treatment in clinic^[2-4]. However, these drugs usually suffer from drawbacks of non-selective biodistribution, undesirable pharmacokinetics and severe side effects including drug resistance after continuous treatment^[5]. Tumor microenvironment (TME)

收稿日期: 2019-09-03。收修改稿日期: 2019-09-24。

北京市自然科学基金(No.2182028), 北京师范大学一年级博士生交叉学科研究基金(No.BNUXKJC1803), 国家自然科学基金(No.21541010)和北京师范大学分析测试基金资助项目。

*通信联系人。E-mail: kzwang@bnu.edu.cn

which is characterized by altered functions of proteins and enzymes distributing in extracellular matrix, disordered dynamic networks of blood and lymphatic vessels, and abnormally expressed factors and cells shows significant difference from normal tissues and plays a key role in tumor initiation, progression, metastasis, and drug resistance^[6-7]. For example, studies have revealed that massive excretion of lactate facilitate breast tumor growth and metastasis^[8]; elevated interstitial fluid pressure hampers the transmigration of therapeutic macromolecules, like monoclonal antibodies, from tumor-supplying vessels into tumor interstitium^[9]; adipocytes in TME activate mitochondrial fatty acid oxidation and autophagy to promote the growth and survival of colon cancer cells^[10]. Dysregulation of pH homeostasis is a prominent hallmark of TME, which related to tumor development, invasion and metastasis, and enhanced chemotherapy resistance as well^[11]. These adverse impacts may be caused by the upgraded secretion of cathepsins which commonly reside in the lysosome but secrete from cancer cells in response to extracellular acidification to digest extracellular matrix protein or cleave and activate other proteases involved in tumor invasion and metastasis^[12]. The acidic pH of TME can act as diagnostically and therapeutically important targets for a broad range of cancers and promote the design of a great amount of pH-sensitive probes^[13-14].

A large number of pH-sensitive photosensitizers (PSs) have so far been reported, which display high affinity to apoptosis-associated sub-organelles, such as lysosomes and mitochondria, due to the pH value varying in different organelles^[15-18] (Fig.1). By virtue of the prominent hallmark of acid TME, pH-activatable materials can respond and amplify pathophysiological signals by overcoming the drawback of high background from the always-on probes, and thus high biological specificity to differentiate tumors from healthy tissues can be achieved^[19]. This high target-to-background ratios (T/B) enable pH-sensitive PSs to become efficient *in vivo* tumor imaging agents. Because of the superior non-invasive character of photodynamic agents, photodynamic therapy (PDT), as

an emerging medical technique, has evolved into a successful alternative or complimentary treatment to some traditional therapeutic methods (*e.g.* radiotherapy, chemotherapy and tumor surgical resection) to fight against cancer^[20-22]. Upon irradiation, PSs can produce highly cytotoxicity reactive oxygen species (ROS), particularly $^1\text{O}_2$ which has a short lifetime and small action radius, to induce cell damage and apoptosis^[23]. pH-responsive PDT can highly enhance the efficacy of tumor therapy through local delivery PSs to acidic tumor lesions together with an appropriate light irradiation^[24-26].

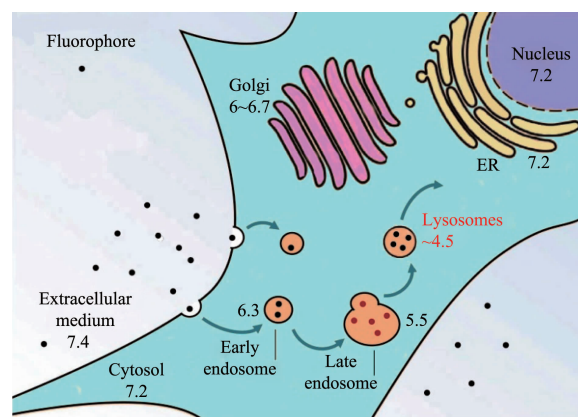


Fig.1 pH values in different organelles

The nanotechnology-based medicines display many advantages of prolonged circulation lifetime, improved biodistribution and up-regulated intratumoral accumulation, and have attracted tremendous attention for tumor imaging, drug delivery and cancer therapy, but their high polydispersity reduce the repeatability of pharmacokinetic behavior^[27-30]. Metal complexes can overcome the aforementioned drawbacks of nanomedicines due to their high homogeneity and attractive photoluminescent properties, making them promising and important candidates for biomedical applications^[31-33]. Compared to traditional tumor imaging drugs, metal complexes have shown good chemical and photochemical stabilities, excitation and emission in visible/near-IR window, high luminescence quantum yields and relatively long lifetimes (τ at μs level) which can reduce effects of autofluorescence (τ at ns level) from biological samples^[34]. A great number of metal complexes have been demonstrated to target cellular

nucleus and various organelles, including the lysosome, mitochondrion, endoplasmic reticulum and Golgi apparatus^[35]. In addition, a large number of metal complexes can act as PSs used for PDT against cancer, because they are nontoxic (or low-toxic) in dark while highly cytotoxic upon irradiation caused by the generation of $^1\text{O}_2$ ^[36-38]. Poynton et al.^[39] summarized the recent development of ruthenium(II) polypyridyl complexes and conjugates for applications as cellular imaging and diagnostic agents. Some pH-responsive moieties, such as imidazo, endow these metal complexes with tumor targeting properties and facilitate highly precise cancer diagnosis and treatment^[40].

Compared to “always-on” fluorescence probes, activatable fluorescence probes that respond and amplify pathological parameters stimuli, can provide specific and sensitive disease detection by greatly improve the T/B. So far, there have been many reviews about stimuli-responsive fluorophores and their biomedical applications, but most of them focused on nanoparticles. Zhou et al. reviewed the recent development of stimuli-responsive polymeric micelles, which are capable of responding biological stimuli such as acidic pH, altered redox potential and upregulated enzyme, and their applications in anticancer drugs delivery, diagnostic and therapeutic drugs^[5]. Li et al. discussed biomedical applications of stimuli-responsive fdNA-NPs which were prepared by integrating inorganic and organic NPs with functional DNA (fdNA, *e.g.* aptamers, DNazymes and aptazymes)^[41]. Similar to these fdNA-NPs, stimuli-responsive DNA-based hydrogels and their applications are summarized by Kahn et al., including controlled drug delivery, sensing, information storage and inscription^[42]. Wang et al. summarized the classification of pH-responsive fluorescence nanoprobe and their applications in tumor imaging^[43]. Nevertheless, to date, there haven't been any reviews focused on pH-sensitive metal complexes for tumor bioimaging and therapy^[44-45]. In this review, we discuss the potential mechanisms of the acidification in TME, and provide some representative entities of pH sensitive fluorescence imaging and tumor therapy based on iridium, ruthenium and

platinum complexes (Fig.2~4).

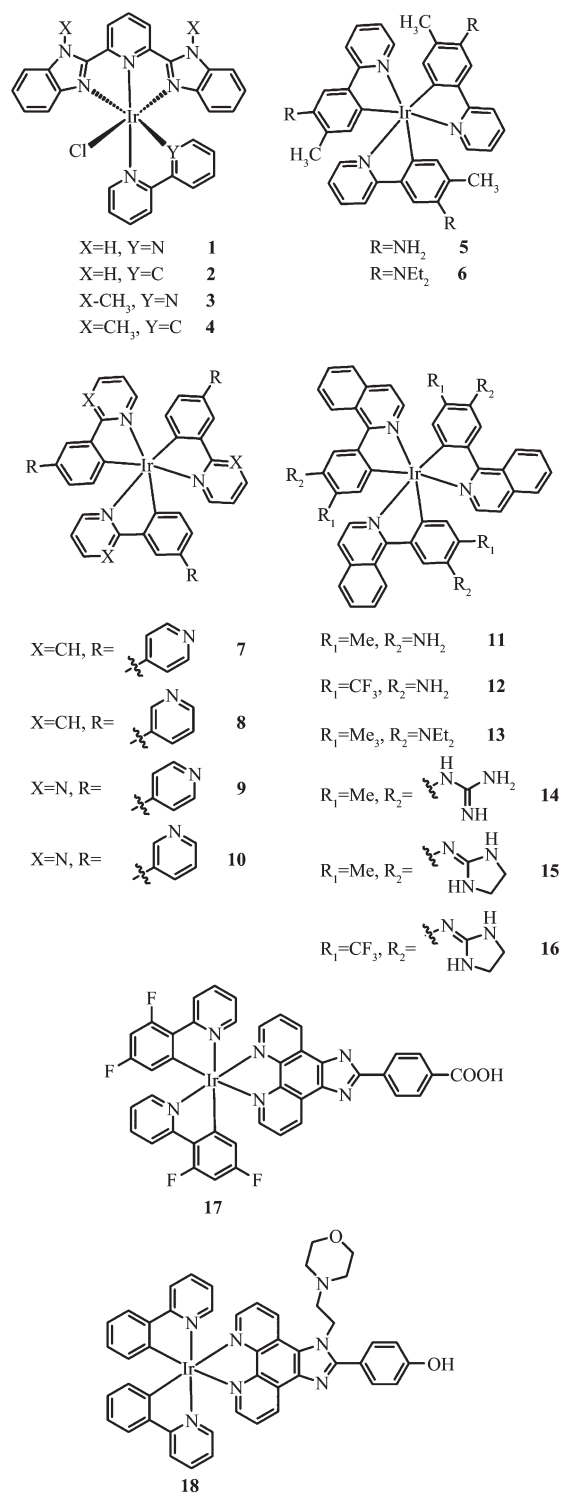


Fig.2 Molecular structures of pH responsive Ir complexes

1 Mechanisms involved in acidification of TME

In what follows, we will discuss the acidic metabolites and the exchangers involved in pH

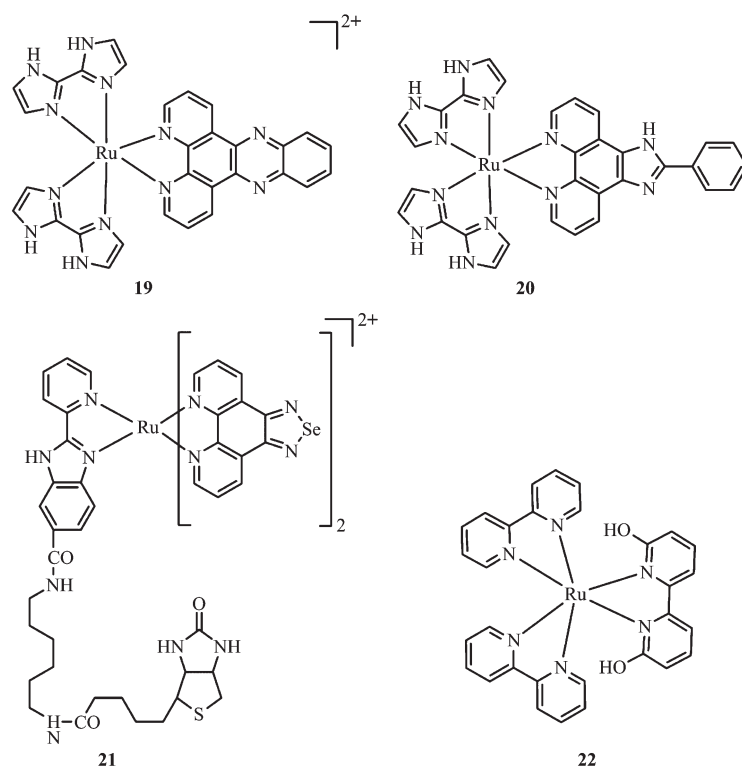


Fig.3 Molecular structures of pH responsive Ru complexes

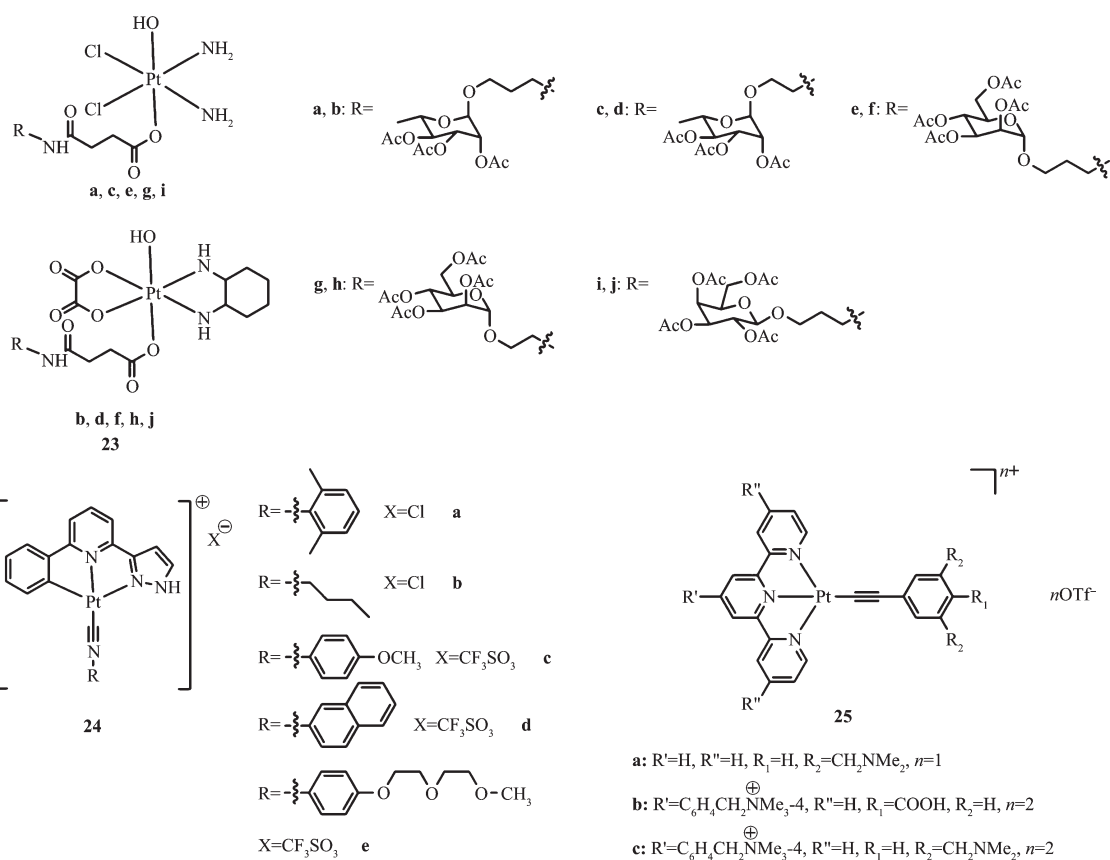


Fig.4 Molecular structures of pH responsive Pt complexes

regulation progress of cancer cells, which induce a consistent acidification of TME.

1.1 Acidic metabolites

Otto Warburg stated the theory that tumor prefer aerobic glycolysis to produce lactate instead of oxidative phosphorylation for energy supply even under normoxic conditions about a century ago^[46]. The later converts glucose into carbon dioxide (CO_2) and water (H_2O) and generate 38 ATP, while the former produce lactate via anaerobic fermentation and the total energy gain is only 2 ATP per glucose molecule^[47]. Although have a poor energy efficiency, anaerobic glycolysis as a faster energy supplier confer a proliferative advantage over TCA for increased biosynthesis, especially in the appearance of metabolic impairment of the oxidative phosphorylation resulting from the intermittent hypoxia in tumor tissues^[48-49]. The glycolytic rate is generally observed to upregulate about 200 times higher in some rapidly growing cancer cells than normal cells, even under conditions where oxygen is available and we called this process “aerobic glycolysis”. The lactic acid has been regarded as the leading metabolites inducing the acidification of TME^[50]. Besides the glycolytic pathway, the up-regulated non-glucose-dependent pathway glutaminolysis in cancer cells also produce lactate to lower extracellular pH (pHe)^[51] than intracellular pH (pHi).

CO_2 produced by pentose phosphate pathway (PPP) is considered to be an alternative cause of intratumoral acidosis. Numerous of studies have confirmed the up-regulation of PPP and a high expression level of related enzyme system in various tumors^[52]. The hypoxia-associated carbonic anhydrase isoforms (CA II, CA IX and CA XII) are widely distributed and can form H^+ and HCO_3^- by reversible catalyzing hydration of CO_2 ($\text{H}_2\text{O} + \text{CO}_2 \rightleftharpoons \text{H}^+ + \text{HCO}_3^-$)^[50,53]. These protons (H^+) are produced extracellularly resulting in the acidification of pHe, which facilitate tumorigenesis.

1.2 pH-regulating exchangers

In normal cells, the pHe is higher than pHi, but it become more acidic extracellularly and more alkaline intracellularly in cancer cells^[54-55]. The reversed

intra-extracellular pH provides a strong mitogenic signal promoting the proliferation of cancer cells bypassing most inhibitory signals, and thus becomes a hallmark of neoplastic tissue^[56]. To develop and maintain such a reversed transmembrane pH gradient, some membrane-based ion exchangers are required.

The reversed pH gradient between the alkaline cytosol and the acidic extracellular environment is driven primarily by the activation of Na^+/H^+ exchanger isoform 1 (NHE1) during transcription which is the earliest step of neoplastic progression^[57]. NHE1 belongs to the secondary active acid extruders family whose responsibility is to extrude intracellular proton (H^+) in a 1:1 electroneutral exchange for extracellular sodium (Na^+)^[11]. In normal cells, NHE1 is believed to function as pHi “house-keeper”, because it can be activated by intracellular acidification to keep pHi homeostasis. In cancer cells, the increased affinity of the proton-regulatory site upsets this balance and hyperactivates NHE1, leading to an increase in pHi and a decrease in pHe. Subsequently, such a pH change directly stimulates the aerobic glycolysis to excrete lactate^[54]. As glycolysis is highly activated in malignant tumors, it is crucial to extrude massive amounts of lactate out of cells to assure a continuous flux of glycolysis and avoid intracellular acidification. MCTs are responsible for controlling pHi and directing lactate flux across the plasma membrane through shuttling glycolysis-related mono-carboxylic acids, namely lactate, pyruvate, and ketone bodies^[58-60]. Therefore, overexpressed MCTs is observed in the majority of cancer cells. The vacuolar H^+ -ATPases (V-ATPases), as a ATP dependent H^+ pump discovered in the early 1980s, generally reside in acidic organelles or the plasma membrane of cancer cells^[61-62]. This proton pump is commonly under tight density control and plays an essential role in controlling the pH of intracellular compartments, cytoplasm, and the extracellular space within normal physiological pH ranges, however in cancer tissues, the overexpression of V-ATPase probably leads to an extracellular pH drift towards acidity and shows a positive correlation with the tumor progression, invasiveness, spread and chemoresistance^[63-64].

Substantial evidences have shown that tumor cells with different metastatic behaviors preferentially carry out different transporting mechanisms^[65]. For example, cancer cells with poorly metastatic potential prefer to activate NHE1, but the plasma membrane H⁺-ATPase shows higher levels than other ion exchangers in highly metastatic cells^[61,66].

2 pH-sensitive metal complexes and their applications in tumor imaging and therapy

Transition metal complexes based on Ir, Ru and Pt have attracted tremendous attention due to their favorable properties including diverse molecular structures, large Stokes shifts, good photostability, and desirable singlet oxygen generation yield^[67-69]. In recent years, researchers have focused on the stimuli-responsive ability of those metal complexes with special moieties. Generally speaking, metal complexes incorporating protonatable or deprotonatable subgroups (*e.g.* imidazole^[70-72], *n*-benzoylthiourea^[73], amine^[74-76] and carboxyl^[77]) are expected to switch the excited states responding to pH change. Particularly, these protonatable/deprotonatable moieties positioned closer to center metal are proved to have larger effect on pH sensitivity in absorption spectra^[73]. It is well known that the emissions of metal complexes can be effectively quenched by molecular oxygen and generate ¹O₂. These pH-sensitive metal complexes can not only promote the precision of tumor imaging but also act as PSs providing the potential to kill cancer cells through PDT.

2.1 Iridium-based complexes

Zheng and coworkers^[21] have reported a series of mixed-ligand phosphorescent Ir(III) complexes **1**~**4** that exhibited high luminescence quantum yields, long phosphorescence lifetimes, and high singlet oxygen quantum yield. They found that **1** and **2** have pH-sensitive emission properties with an increased quantum yield of about 6- and 5-fold when pH value changes from neutral (7.4) to acidic (3.0). In addition, **2** and **4** showed high cellular uptake efficiency through an energy-dependent mechanism, and can

specifically image lysosomes and mitochondria, respectively. Upon irradiation (425 nm, 36 J·cm⁻²), moderate phototoxicities were observed in both **2** and **4** against Hela, MCF-7, A549 and A549R. The Ir(III) complex **2** displayed the highest phototoxicity index (PI>54) in A549 cells. The mechanism investigation of PDT effects indicated that **1** and **2** can induce apoptosis by ROS generation (Fig.5a) and caspase activation (Fig.5b) under visible light.

Shinsuke and coworkers^[75-76] reported two pH-sensitive cyclometalated Ir(III) complexes **5** and **6** that can act as pH-dependent on-off fluorescent probes because their emissions were almost silent under neutral to basic conditions but considerably enhanced under acidic conditions (Fig.6). The complex **6** is capable of selectively staining acidic organelle of lysosome and producing ¹O₂ in a pH-dependent manner. PDT phenomenon was observed when treated Hela cells with complex **6**. Similar structures (**7**~**10**) reported by Akihiro et al.^[78] presented comparable properties. Compared with **6**, complex **7** (1) exhibited similar pH-dependent photochemical behavior of large Stokes shift (>50 nm) upon acidification; (2) generated ¹O₂ more efficient and faster; (3) localized in mitochondria rather than lysosomes and emitted a green color in deprotonated form; (4) induced necrosis-like cell death more efficiently.

A series of pH-activatable Ir(III) complexes (**11**~**16**) with red-emitting property upon acidification were reported by Kando^[79]. Co-staining studies demonstrated that **16** is an optimal probe for sensitive staining of lysosomes among these red-emitting Ir(III) complexes in this work. **15** and **16** were taken up by cells through a passive transport mechanism and induce the necrosis like cell death upon photoirradiation at 465 nm.

Many reported transition metal complexes have prominent properties but poor aqueous solubility greatly limit their further exploration in the biological fields. Conjugating with hydrophilic groups is an efficient method to improve their biocompatibility. Dolan et al.^[80] reported a pH-sensitive Ir(III) complex **17** and its octaarginine conjugate. They studied and compared the cell uptake and cytotoxicity of the

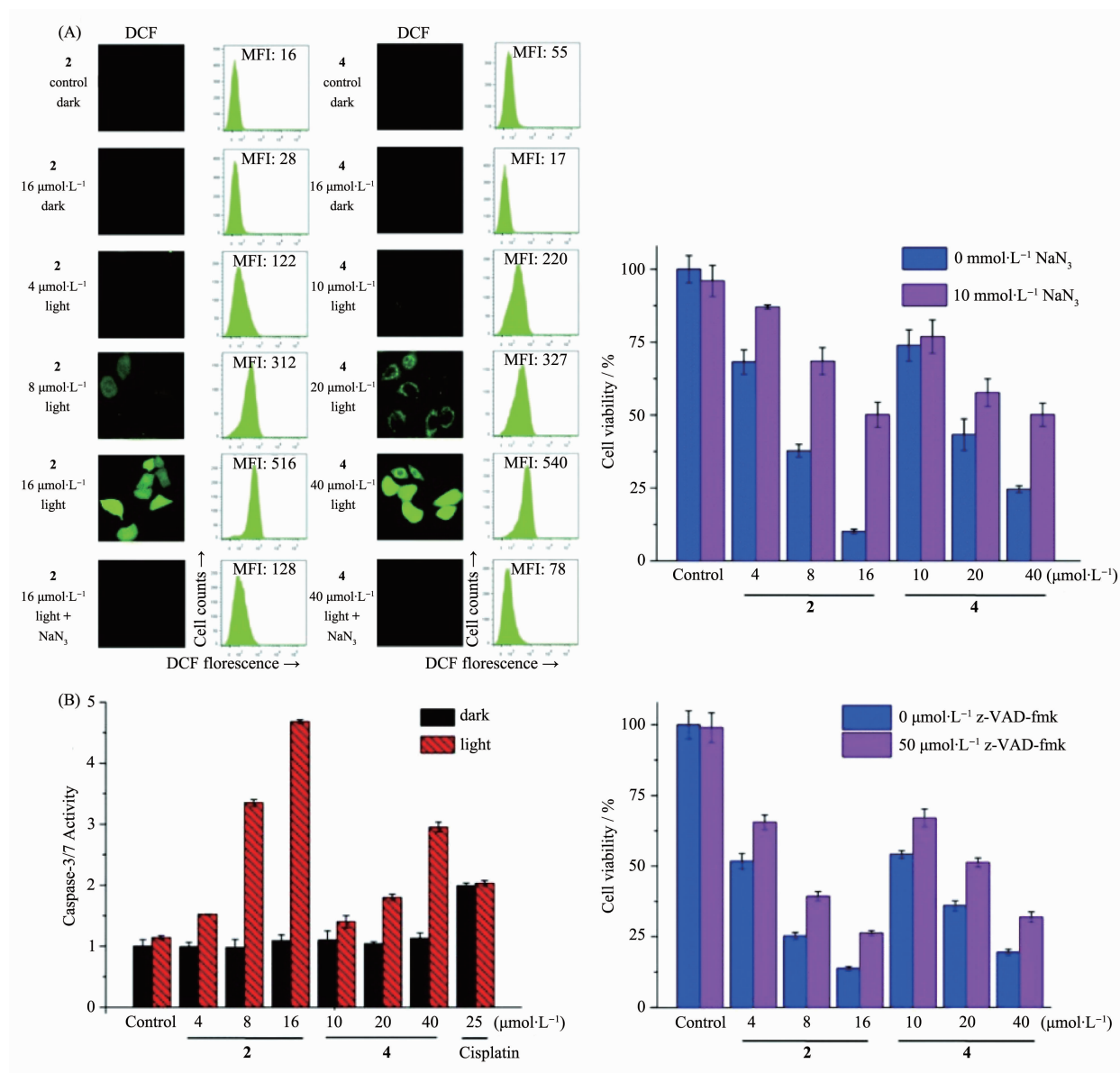


Fig.5 (a) Detection of intracellular ROS produced by **2** and **4** upon irradiation (left) and impact of ROS inhibitor of NaN_3 on cytotoxicity of **2** and **4** after PDT treatment (right); (b) Caspase-3/7 activity after **2** and **4** treated A549 cells in the absence or presence of light (left) and cytotoxicity of **2** and **4** under irradiation (425 nm) against A549 cells with the presence of pan-caspase inhibitor of z-VAD-fmk (right)^[21]

parent Ir(III) complex **17** and its conjugate in myeloma (SP2) and Chinese hamster ovary (CHO) cell lines. They found that the conjugation rendered the complex better water solubility, higher dark (and light) cytotoxicity and stronger membrane permeability. Confocal imaging indicated the conjugate can penetrate the nucleus, which may result in high cytotoxicity. Liu et al.^[81] designed a pH-sensitive Ir(III) complex (**18**) which exhibited large Stokes shift, good photostability and long lifetime. The incorporation of

hydroxy groups in its structure endowed this complex highly water-soluble. When pH increased, the luminescent intensity of this hydrophilic Ir(III) complex was significantly reduced. This is because the introduction of morpholine group (pH=5~6) quenches the luminescence of Ir center through photoinduced electron transfer (PET) in neutral to basic conditions and convert to protonated form in acidic conditions leading to an enhancement of luminescence emission. These properties make complex **18** an excellent

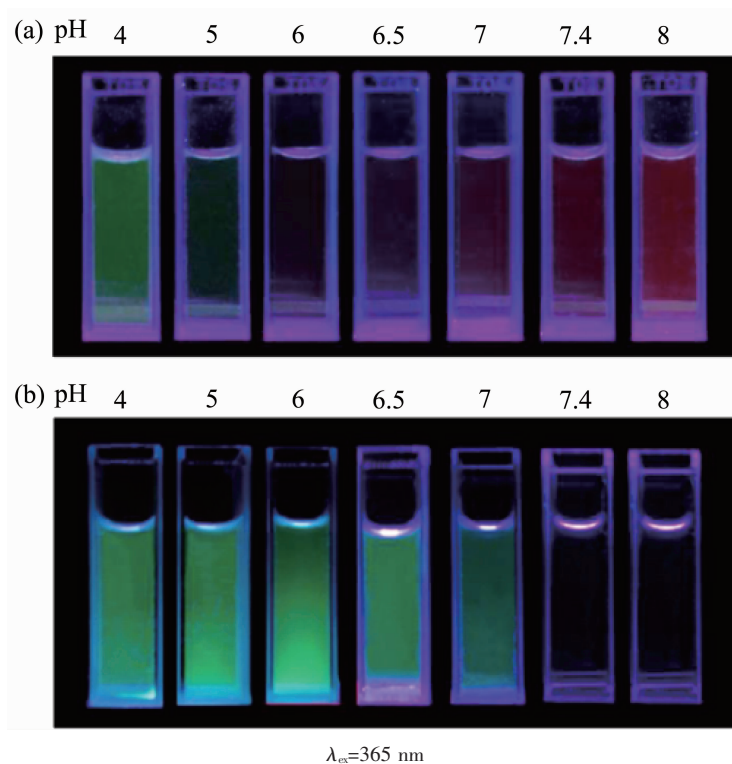


Fig.6 Photograph showing the pH-dependent behaviors of **5** (a) ($100 \mu\text{mol}\cdot\text{L}^{-1}$) and **6** (b) ($1 \mu\text{mol}\cdot\text{L}^{-1}$) in degassed DMSO/ $100 \text{ mmol}\cdot\text{L}^{-1}$ buffer (pH=4~8)^[76]

luminescent probe for visualizing lysosomes in cancer cells.

2.2 Ruthenium-based complexes

Compared with fluorescence imaging in visible spectrum, newly emerging fluorescence imaging technique in the near-infrared window (NIR, $700\sim 1\,000 \text{ cm}^{-1}$) has been demonstrated considerable advantages, including minimized autofluorescence, reduced optical scattering and absorption of tissues, which facilitate deep anatomical visualization in clinical diagnosis and surgical interventions guide. Yu et al.^[82] reported two Ru(II) complexes (**19**~**20**) that responded sensitively to pH in solution and living cells. With the increase of pH value from 1.88 to 11.7, the MLCT peak of complex **19** displayed a significant red-shift from 462 to 527 nm accompanying with the color of the solution changing from yellow to purple, indicating that the complex **19** can be served as a naked-eye colorimetric probe for pH detection. Complex **20** was non-fluorescent in basic to neutral condition, while emitted a bright fluorescence (~ 400 -fold) at a near-infrared wavelength upon the pH value decrease to 1.88. Similar

phenomenon was observed in living cells. Confocal imaging study revealed that complex **19** localized at lysosomes and sensitively monitored the change of pH in lysosomes making it a promising lysosomes pH sensor during physiological and pathological processes.

It has been well-documented that selenium (Se)-containing compounds exhibit outstanding anticancer potency, but the poor solubility and undesirable luminescent properties limit their applications *in vivo*^[83-84]. Conjugating Se-based compounds with metal complexes has been proved to be an effective strategy to solve this problem^[85-86]. Zhao et al.^[87] developed a Se-containing Ru complex (Ru-BSe, **21**) and demonstrated its application as a potential theranostic drug for tumor diagnosis and therapy. This complex can be specifically internalized by tumor tissue and then rapidly decompose to release therapeutic complex under weakly acidic TME. The Ru-BSe possessed high specificity to mitochondria and triggered mitochondrial dysfunction and intrinsic apoptosis through ROS-mediated endoplasmic reticulum stress signal pathway. The *in vivo* and *ex vivo* imaging examination

indicated that compared to Ru-Se (without target unit), Ru-BSe can specifically accumulate in the tumor site within 72 h intravenous injection, and the Ru content in Ru-BSe-treated tumor was much higher than that of normal tissues (Fig.7).

Photo-driven activation of platinum complexes as anticancer agents is attractive and has been demonstrated to be a success^[88-89]. Recently, Glazer and co-workers^[90] realized light induced anti-cancer activity in ruthenium polypyridyl complexes. In this class of complexes, 6,6'-dimethyl-2,2'-bipyridine (66' bpy (Me)₂) are served as the photo-dissociation ligand, and after dissociation, and the cytotoxicity of these complexes are highly enhanced. Based on Glazer's work, Hufziger used the pH sensitive ligand, 6,6' -

dihydroxy-2,2'-bipyridine (66' bpy(OH)₂), to develop a ruthenium dihydroxybipyridine complex [Ru(bpy)₂(66' bpy(OH)₂)]²⁺ (**22**) that can be exploited as a photo-induced anti-cancer prodrug^[91]. The Ru-N bond lengths in 66' bpy (OH)₂ complex are longer than that in polypyridyl complexes without 6 and 6' substitution, leading to a weaker bond of the ligand to the metal center. Therefore, upon irradiation at low pH value, the protonated complex suffered from a photo-dissociation of the pH-sensitive 66' bpy (OH)₂ ligand from the complex. Due to the cytotoxicity of 66' bpy (OH)₂, this photo-induced dissociation process convert non-toxic [Ru(bpy)₂(66' bpy(OH)₂)]²⁺ to cytotoxic agents in acid TME and thus exhibit the possibility to realize targeted tumor therapy.

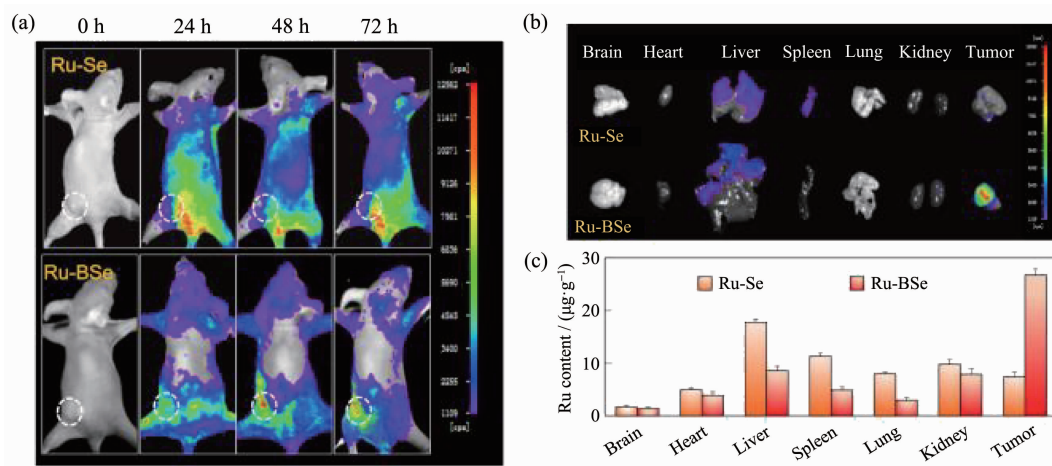


Fig.7 Precise tumor diagnosis of Ru-BSe *in vivo*: (a) Real-time monitoring the accumulation and distribution of Ru-Se and Ru-BSe (4 μmol·kg⁻¹) in Hela xenografts nude mice at different time points; (b) *Ex vivo*-dissected organs (brain, heart, liver, spleen, lung, kidney, and tumor tissue) fluorescent images of Ru-Se and Ru-BSe after 72 h tail vein injection; (c) Biodistribution of Ru in main organs after 30 days treatment of Ru-BSe in Hela xenografts nude mice using ICP-AES^[88]

2.3 Platinum-based complexes

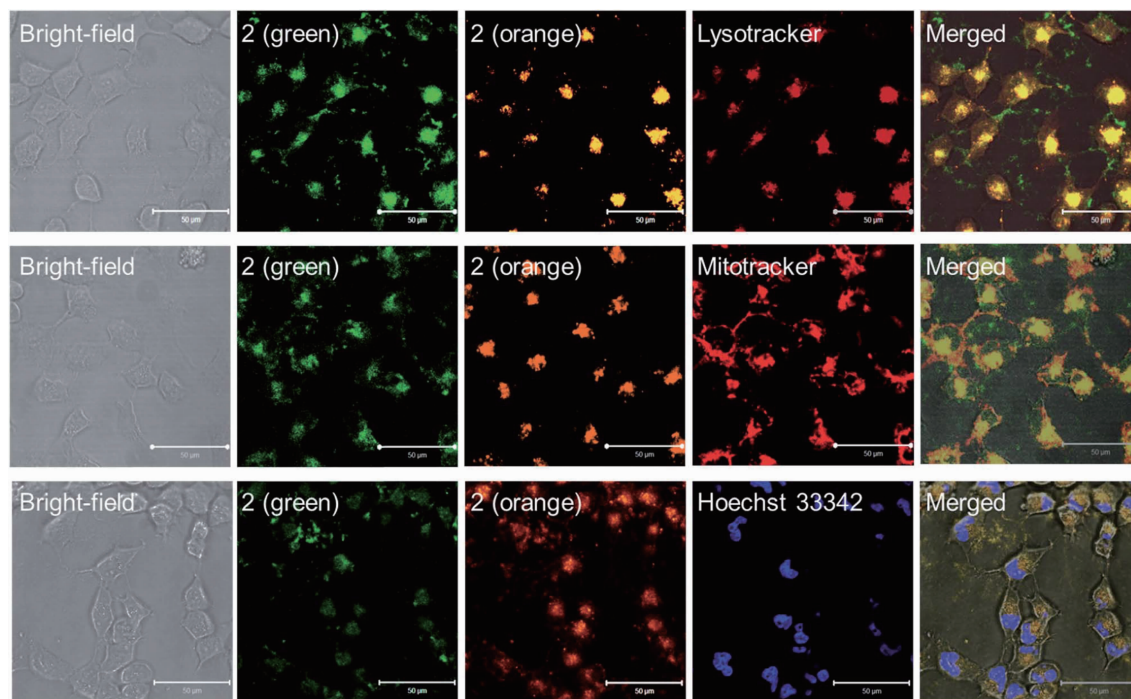
Platinum(II)-based anticancer drugs possess both efficacy and undesirable side effects due to their inherent reactivity with DNA. Cisplatin, for example, performs its anticancer activity by the formation of cross-links with nucleic acids blocking the DNA replication and transcription. The “off-target” effects, however, result in drug-induced toxic and side effects and the little margin between treatment dose and toxic dose^[90]. Platinum(IV) prodrugs remain inert in biological fluids, but regain their cytotoxicity when encounter

reductants like glutathione and ascorbic acid. Therefore, tuning the chemical properties of platinum (IV) complexes to reduce the possibility of reduction in the blood stream before reaching the cancer sites becomes a key point to improve the therapeutic efficacy of platinum(II)-based anticancer drugs^[92-93]. Ma et al.^[94] designed and synthesized a series of carbohydrate-conjugated platinum(IV) complexes (**23a~j**) based on the clinical anticancer drugs cisplatin and oxaliplatin. By virtue of the pH and redox dual-responsive properties and the higher uptake of

carbohydrate by cancer cells than healthy non-cancerous cells, the prepared carbohydrate-conjugated platinum (IV) complexes exhibited more potent cytotoxicity in seven tested cancer cells and lower toxicity to normal cells than cisplatin and oxaliplatin. More importantly, they displayed a positive shift of reduction properties at pH 6.4, which facilitate the tumor targeted therapy. The *in vivo* studies indicated that these complexes could efficiently inhibit the growth of MCF-7 tumor and have potential safety of high-dose treatment.

In recent years, self-assembly of organometallic complexes driven by intermolecular metal-metal interaction have been actively studied in materials science and have inspired a surge of interest on their biomedical applications^[95]. This interaction can endow complexes tunable optical, intriguing electrochemical properties and desirable biological activities. Tsai and coworkers reported a series of Pt(II) complexes (**24a~e**) containing pincer type ligands^[96]. All of these complexes displayed pH-dependent self-assembly and accom-

panied red-shifted in emission spectra from orange to green. The specific cellular location of **24b** examined by confocal microscopy demonstrated that upon excitation at 458 nm, the green emission (monomeric form) and orange emission (aggregated form) from **24b** exhibited co-localization with the red signal from LysoTracker Red showing Pearson's coefficients $R = 0.60$ and 0.75 , respectively, but almost no overlap with mitochondria and nuclei signals ($R < 0.15$) were observed (Fig.8). Importantly, this accumulation can lead to increased lysosomal membrane permeability and induce cell apoptosis. The complex **24a** can form hydrogels in water and displayed low-pH-stimulated and time-dependent anticancer activities. Moreover, these hydrogels can also function as anticancer drugs delivery vehicles realizing dual therapeutic effects. Chung and co-workers^[97] conducted a similar study, in which a series of water-soluble pH-responsive Pt(II) terpyridine complexes (**25a~d**) have been designed and synthesized, and some of them displayed pH-induced self-assembly and disassembly in aqueous



Lysotracker Red DND-99: $50 \text{ nmol} \cdot \text{L}^{-1}$, $\lambda_{\text{ex}}=543 \text{ nm}$, $\lambda_{\text{em}}=565\sim615 \text{ nm}$; Mitotracker: $50 \text{ nmol} \cdot \text{L}^{-1}$, $\lambda_{\text{ex}}=543 \text{ nm}$, $\lambda_{\text{em}}=565\sim615 \text{ nm}$; Hoechst 33342: $1 \mu\text{mol} \cdot \text{L}^{-1}$, $\lambda_{\text{ex}}=800 \text{ nm}$ (two photon), $\lambda_{\text{em}}=435\sim485 \text{ nm}$; Complexes **24b** (green) and **24b** (orange) are both excited at 458 nm but with emission channels of 500~550 nm and 650~700 nm, respectively

Fig.8 Selective imaging of lysosomes (top), mitochondria (middle) and Hoechst 33342 (bottom) by **24b** ($10 \mu\text{mol} \cdot \text{L}^{-1}$) in HeLa cells analyzed by confocal microscopy^[97]

media resulting in remarkable UV-Vis absorption and emission spectral changes. Fluorescent confocal imaging experiments indicated the potential of this class of complexes as pH-responsive NIR probes to differentiate lysosome from other cellular organelles.

3 Outlook

Inspired by the unique and fascinating hallmark of acidic tumor microenvironment, much attention has focused on the design of pH-responsive fluorescence probes based on varieties of materials, such as organic and inorganic dyes, biomaterials and synthetic polymers, among which metal complexes have become a prominent category. Although numerous pH sensors based on Ir, Ru and Pt complexes have been reported and exhibited attractive optical properties and good behaviors in bio-imaging and tumor therapy applications, there also exist some problems required to be dealt with.

(1) Some pH-sensitive metal complexes suffer from poor aqueous solubility resulting in the low membrane penetrability, and therefore most of them are limited in organic solution-based researches. Therefore, improving their aqueous solubility and biocompatibility hold the key to expanding their applications in biological field. A common method is that use DMSO as co-solvent to facilitate the transmembrane transport of metal complexes, because DMSO is an ideal solvent for almost all transition metal complexes and it has the ability to alter the cell permeability^[81]. An alternative solution would be modification with hydrophilic and functional groups to improve their hydrophilicity.

(2) Some pH sensitive metal complexes display two-photon excitation (*ca.* 800 nm) or NIR emission properties which facilitate deep-penetration imaging and therapy *in vivo*. It is desirable to design and synthesis novel pH-sensitive metal complexes with excitation and emission wavelengths in NIR window.

(3) Although several researches of pH-sensitive probes have focused on the combination of PDT with chemotherapy to overcome the limitation of single treatment approach against cancer, the outcome

remains unsatisfactory for curing cancer thoroughly. Therefore, triple or even more modes of combinatorial therapy are required to improve the synergistic anticancer efficacy and minimize side effects of pH-sensitive metal complexes.

(4) As an increasing number of *in vitro* and *in vivo* researches have been conducted and indicated some inspiring outcomes, more efforts are need to explore the toxicology and pharmacology of this class of pH-sensitive metal complexes, which will become invaluable in the future applications in clinical cancer diagnosis and therapy.

References:

- [1] Qiu K Q, Wang J Q, Song C L, et al. *ACS Appl. Mater. Interfaces*, **2017**,**9**(22):18482-18492
- [2] Ganipineni L P, Danhier F, Préat V. *J. Controlled Release*, **2018**,**281**:42-57
- [3] Wang C S, Wang Z H, Zhao T, et al. *Biomaterials*, **2018**,**157**: 62-75
- [4] Tringale K R, Pang J, Nguyen Q T. *WIREs Syst. Biol. Med.*, **2018**,**10**(8924):e1412
- [5] Zhou Q, Zhang L, Yang T H, et al. *Int. J. Nanomed.*, **2018**, **13**:2921-2942
- [6] Wang M N, Zhao J Z, Zhang L S, et al. *J. Cancer*, **2017**,**8**(5): 761-773
- [7] Romero-Garcia S, Moreno-Altamirano M M B, Prado-Garcia H, et al. *Front. Immunol.*, **2016**,**7**:52
- [8] Li L, Kang L, Zhao W, et al. *Cancer Lett.*, **2017**,**400**:89-98
- [9] Hofmann M, Pflanzner R, Habib A, et al. *Transl. Oncol*, **2016**,**9** (3):179-183
- [10] Wen Y A, Xing X P, Harris J W, et al. *Cell Death Dis.*, **2017**, **8**(2):e2593
- [11] Amith S R, Fliegel L. *Semin. Cancer Biol.*, **2017**,**43**:35-41
- [12] Hinton A, Bond S, Forgac M. *Pfluegers Arch. Eur. J. Phys.*, **2009**,**457**(3):589-598
- [13] Liu Z P, Zhang C L, He W J, et al. *New J. Chem.*, **2010**,**34** (4):656-660
- [14] Chen Y C, Zhu C C, Cen J J, et al. *Chem. Sci.*, **2015**,**6**(5): 3187-3194
- [15] Chen X H, Chen Z W, Hu B H, et al. *Small*, **2018**,**14**(9): 1703164
- [16] Shen S L, Zhang X F, Ge Y Q, et al. *Sens. Actuators B*, **2018**,**256**:261-267
- [17] Hong K I, Park S H, Lee S M, et al. *Sens. Actuators B*,

- 2019,286**:148-153
- [18]Zhao X J, Chen Y, Niu G Y, et al. *ACS Appl. Mater. Interfaces*, **2019,11**(14):13134-13139
- [19]Yuan P, Ruan Z, Li T W, et al. *Nanomed-Nano. Technol.*, **2019,15**(1):198-207
- [20]Dickerson M, Sun Y, Howerton B, et al. *Inorg. Chem.*, **2014, 53**(19):10370-10377
- [21]Zheng Y, He L, Zhang D Y, et al. *Dalton Trans.*, **2017,46** (34):11395-11407
- [22]Martinez M A, Carranza M P, Massaguer A, et al. *Inorg. Chem.*, **2017,56**(22):13679-13696
- [23]Rosca C Y, Horlescu P, Stan C S, et al. *Turk. J. Chem.*, **2017,41**(5):648-657
- [24]Li F Y, Du Y, Liu J A, et al. *Adv. Mater.*, **2018,30**(35): 1802808
- [25]Yang G B, Xu L G, Xu J, et al. *Nano Lett.*, **2018,18**(4):2475 -2484
- [26]Xia F F, Hou W X, Zhang C L, et al. *Acta Biomater.*, **2018, 68**:308-319
- [27]Danaei M, Dehghankhold M, Ataei S, et al. *Pharmaceutics*, **2018,10**(2):57
- [28]Urandur S, Banala V T, Shukla R P, et al. *ACS Appl. Mater. Interfaces*, **2018,10**(15):12960-12974
- [29]Cai Y, Wei Z, Song C H, et al. *Chem. Soc. Rev.*, **2019,48** (1):22-37
- [30]Wang Y G, Zhou K J, Huang G, et al. *Nat. Mater.*, **2014,13** (2):204-212
- [31]Kando A, Hisamatsu Y, Ohwada H, et al. *Inorg. Chem.*, **2015,54**(11):5342-5357
- [32]Zhang S J, Hosaka M, Yoshihara T, et al. *Cancer Res.*, **2010, 70**(11):4490-4498
- [33]Zhang P Y, Huang H Y, Chen Y, et al. *Biomaterials*, **2015, 53**:522-531
- [34]Fernández-Moreira V, Thorp-Greenwood F L, Coogan M P. *Chem. Commun.*, **2010,46**(2):186-202
- [35]Qiu K Q, Chen Y, Rees T W, et al. *Coord. Chem. Rev.*, **2019,378**:66-86
- [36]Zhou Z X, Liu J P, Rees T W, et al. *Proc. Natl. Acad. Sci. U.S.A.*, **2018,115**(22):5664-5669
- [37]Zhao X Z, Li M L, Wen S, et al. *Chem. Commun.*, **2018,54** (51):7038-7041
- [38]Liu Y, Hammit R, Lutterman D A, et al. *Inorg. Chem.*, **2008, 48**(1):375-385
- [39]Poynton F E, Bright S A, Blasco S, et al. *Chem. Soc. Rev.*, **2017,46**(24):7706-7756
- [40]Meng T T, Xue L X, Wang H, et al. *J. Mater. Chem. C*, **2017, 5**(13):3390-3396
- [41]Li L L, Xing H, Zhang J J, et al. *Acc. Chem. Res.*, **2019,52** (9):2415-2426
- [42]Kahn J S, Hu Y W, Willner I. *Acc. Chem. Res.*, **2017,50**(4): 680-690
- [43]Wang L, Li C. *J. Mater. Chem. C*, **2011,21**(40):15862-15871
- [44]Feng L Z, Dong Z L, Tao D L, et al. *Natl. Sci. Rev.*, **2017,5** (2):269-286
- [45]Zheng H Q, Xing L, Cao Y Y, et al. *Coord. Chem. Rev.*, **2013,257**(11/12):1933-1944
- [46]Warburg O, Wind F, Negelein E. *J. Gen. Physiol.*, **1927,8** (6):519-530
- [47]Tennant D A, Durán R V, Gottlieb E. *Nat. Rev. Cancer*, **2010,10**(4):267-277
- [48]Gatenby R A, Gillies R J. *Nat. Rev. Cancer*, **2004,4**(11):891 -899
- [49]De Preter G, Neveu M A, Danhier P, et al. *Oncotarget*, **2016, 7**(3):2910-2920
- [50]Kato Y, Ozawa S, Miyamoto C, et al. *Cancer Cell Int.*, **2013, 13**(1):89
- [51]Böhme I, Bosserhoff A K. *Pigment Cell Melanoma Res.*, **2016,29**(5):508-523
- [52]Gabriel H, Axel S, Marc D, et al. *Clin. Cancer Res.*, **2002,8** (4):1284-1291
- [53]Gallagher F A, Helen S, Kettunen M I, et al. *Cancer Res.*, **2015,75**(19):4109-4118
- [54]Stubbs M, Mcsheehy P M J, Griffiths J R, et al. *Mol. Med.*, **2000,6**(1):15-19
- [55]Parks S K, Johanna C, Jacques P. *Nat. Rev. Cancer*, **2013, 13**(9):611-623
- [56]Schwartz L, Supuran C T, Alfarouk K O. *Anti-Cancer Agents Med. Chem.*, **2017,17**(2):164-170
- [57]Cardone R A, Valeria C, Reshkin S J. *Nat. Rev. Cancer*, **2005,5**(10):786-795
- [58]Damaghi M, Wojtkowiak J, Gillies R. *Front. Physiol.*, **2013, 4**(370):1-10
- [59]Hée V F V, Labar D, Dehon G, et al. *Oncotarget*, **2017,8** (15):24415-24428
- [60]Pérez-Escuredo J, Hée V F V, Sboarina M, et al. *Biochim. Biophys. Acta*, **2016,1863**(10):2481-2497
- [61]Pérez-Sayáns M, García-García A, Reboiras-López M D, et al. *Int. J. Oncol.*, **2009,34**(6):1513-1520
- [62]Sennoune S R, Luo D, Martinez-Zaguilán R. *Cell Biochem. Biophys.*, **2004,40**(2):185-206
- [63]Spugnini E P, Citro G, Fais S. *J. Exp. Clin. Cancer Res.*, **2010,29**(1):44
- [64]Kulshrestha A, Katara G K, Ibrahim S, et al. *Oncotarget*, **2015,6**(6):3797-3810
- [65]Stefano F, Angelo D M, Haiyan Y, et al. *Cancer Res.*, **2007, 67**(22):10627-10630

- [66]Sennoune S R, Karina B, Martínez G M, et al. *Am. J. Physiol. Cell Physiol.*, **2004**,**286**(6):1443-52
- [67]Sepehrpour H, Fu W X, Sun Y, et al. *J. Am. Chem. Soc.*, **2019**,**141**(36):14005-14020
- [68]Ng W M, Guo X Y, Cheung W M, et al. *Dalton Trans.*, **2019**, **48**:13315-13325
- [69]Rojas Perez Y, Slep L D, Etchenique R. *Inorg. Chem.*, **2019**, **58**(17):11606-11613
- [70]Gao F, Chen X, Zhou F, et al. *Inorg. Chim. Acta*, **2009**,**362** (14):4960-4966
- [71]Gao F, Chao H, Zhou F, et al. *Inorg. Chem. Commun.*, **2007**, **10**(2):170-173
- [72]Gao F, Chen X, Sun Q, et al. *Inorg. Chem. Commun.*, **2012**, **16**(2):25-27
- [73]San S T, Yanagisawa S, Inagaki K, et al. *Phys. Chem. Chem. Phys.*, **2017**,**19**(4):25734-25745
- [74]Karawajczyk A, Buda F. *J. Biol. Inorg. Chem.*, **2005**,**10**(2): 208-208
- [75]Shin A, Yasuki M, Shiori O, et al. *Inorg. Chem.*, **2011**,**50**(3): 806-18
- [76]Shinsuke M, Yosuke H, Toshihiro S, et al. *Inorg. Chem.*, **2016**,**51**(23):12697-12706
- [77]Xia Y M, Wang Y M, Wang Y P, et al. *Colloids Surf. B*, **2011**,**88**(2):674-681
- [78]Akihiro N, Yosuke H, Shinsuke M, et al. *Inorg. Chem.*, **2014**, **53**(1):409-422
- [79]Kando A, Hisamatsu Y, Ohwada H, et al. *Inorg. Chem.*, **2015**, **54**(11):5342-5357
- [80]Dolan C, Moriarty R D, Lestini E, et al. *J. Inorg. Biochem.*, **2013**,**119**(2):65-74
- [81]Liu J B, Vellaisamy K, Li G D, et al. *J. Mater. Chem. B*, **2018**,**6**(23):3855-3858
- [82]Yu H J, Hao Z F, Peng H L, et al. *Sens. Actuators B*, **2017**, **252**:313-321
- [83]Adam A M A. *J. Mol. Struct.*, **2019**,**1195**:43-57
- [84]Aljuhani E. *Russ. J. Gen. Chem.*, **2019**,**89**(5):1042-1050
- [85]Chen Y, Qiao L P, Ji L N, et al. *Biomaterials*, **2014**,**35**(1):2-13
- [86]Deng Z Q, Yu L L, Gao W Q, et al. *Chem. Commun.*, **2015**, **51**(13):2637-2640
- [87]Zhao Z N, Gao P, You Y Y, et al. *Chem. Eur. J.*, **2018**,**24** (13):3289-3298
- [88]Presa A, Vázquez G, Barrios L A, et al. *Inorg. Chem.*, **2018**, **57**(7):4009-4022
- [89]Yulia Yu S D, Legin A A, Jakupc M A, et al. *Inorg. Chem.*, **2011**,**50**(21):10673-81
- [90]Howerton B S, Heidary D K, Glazer E C. *J. Am. Chem. Soc.*, **2012**,**134**(20):8324
- [91]Hufziger K T, Thowfeik F S, Charboneau D J, et al. *J. Inorg. Biochem.*, **2014**,**130**(1):103-111
- [92]Jin S X, Guo Y, Song D F, et al. *Inorg. Chem.*, **2019**,**58**(9): 6507-6516
- [93]Guo Y, Zhang S R, Yuan H, et al. *Dalton Trans.*, **2019**,**48** (11):3571-3575
- [94]Ma J, Yang X D, Hao W P, et al. *Eur. J. Med. Chem.*, **2017**, **128**:45-55
- [95]Wang H, Qiu Z H, Liu H, et al. *Front. Chem.*, **2019**,**7**:39
- [96]Tsai J L L, Zou T T, Liu J, et al. *Chem. Sci.*, **2015**,**6**(7): 3823-3830
- [97]Chung C Y S, Li S P Y, Lo K K W, et al. *Inorg. Chem.*, **2016**,**55**(9):4650-4663